AGU PUBLICATIONS

JGR

Journal of Geophysical Research: Oceans

RESEARCH ARTICLE

10.1002/2015JC011528

Key Points:
- Using field measurements, the vertical variability of K_d(USR) is evaluated
- Relationship between K_d(USR) and K_d(490) is refined to extend its applicability
- Distribution of K_d(USR) of global oceans and its implications are shown

Correspondence to:
J. Lin,
Junfang.Lin@umb.edu

Citation:
Lin, J., Z. Lee, M. Ondrusek, and M. Kahru (2016), Attenuation coefficient of usable solar radiation of the global oceans, *J. Geophys. Res. Oceans*, *121*, 3228–3236, doi:10.1002/2015JC011528.

Received 5 DEC 2015
Accepted 21 MAR 2016
Accepted article online 24 MAR 2016
Published online 20 MAY 2016

Attenuation coefficient of usable solar radiation of the global oceans

Junfang Lin[1], Zhongping Lee[1], Michael Ondrusek[2], and Mati Kahru[3]

[1] Optical Oceanography Laboratory, School for the Environment, University of Massachusetts Boston, Boston, Massachusetts, USA, [2]NOAA/NESDIS Center for Weather and Climate Prediction, College Park, Maryland, USA, [3]Scripps Institution of Oceanography, University of California, San Diego, California, USA

Abstract Usable solar radiation (USR) represents spectrally integrated solar energy in the spectral range of 400–560 nm, a domain where photons penetrate the most in oceanic waters and thus contribute to photosynthesis and heating at deeper depths. Through purely numerical simulations, it was found that the diffuse attenuation coefficient of downwelling USR (K_d(USR), m^{-1}) is nearly a constant vertically in the upper water column for clear waters and most turbid waters. Subsequently an empirical model was developed to estimate K_d(USR) based on the diffuse attenuation coefficient at 490 nm (K_d(490), m^{-1}). We here evaluate this relationship using data collected from a wide range of oceanic and coastal environments and found that the relationship between K_d(490) and K_d(USR) developed via the numerical simulation is quite robust. We further refined this relationship to extend the applicability to "clearest" natural waters. This refined relationship was then used to produce sample distribution of K_d(USR) of global oceans. As expected, extremely low K_d(USR) (~0.02 m^{-1}) was observed in ocean gyres, while significantly higher K_d(USR) (~5.2 m^{-1}) was found in very turbid coastal regions. A useful application of K_d(USR) is to easily and accurately propagate surface USR to deeper depths, potentially to significantly improve the estimation of basin scale primary production and heat fluxes in the upper water column.

1. Introduction

The availability of solar radiation in the upper ocean is important for both physical and biological processes. To quantify this amount of solar energy, conventionally the photosynthetic available radiation (PAR, quanta m^{-2} s^{-1}) has been used [*Kirk*, 1994; *McCree*, 1981], which represents radiant energy in the spectral range of 400–700 nm. In order to study heat transfer and phytoplankton dynamics in the oceans, it is necessary to know the intensity of PAR and its spatial distribution, both horizontally and vertically. In the past decades, a simple expression has been widely used to model the penetration of PAR from surface to depth [*Buiteveld*, 1995; *Kara et al.*, 2005; *Murtugudde et al.*, 2002; *Paulson and Simpson*, 1977], which is commonly expressed as:

$$PAR(z)=PAR(0^-)\cdot\exp\left[-K_d(PAR)\cdot z\right] \quad (1)$$

where $PAR(0^-)$ is the PAR value just beneath the water surface, and K_d(PAR) (m^{-1}) is the diffuse attenuation coefficient of PAR.

Although $PAR(0^-)$ and K_d(PAR) of the oceans have been produced as stand-alone products from satellite ocean color remote sensing [*Frouin and Pinker*, 1995; *Frouin et al.*, 2012; *Wang et al.*, 2009], numerous studies have shown that K_d(PAR) cannot be treated as a depth-independent property [*Lee*, 2009; *Morel*, 1988; *Smith et al.*, 1989]. *Lee* [2009] showed that K_d(PAR) of oceanic waters will vary by almost three folds from surface to the bottom of the euphotic zone due to the strong absorption by water molecules in the longer wavelengths. Thus, significant errors in the estimation of PAR at depth would be resulted if a vertically constant K_d(PAR) is used, and subsequently inaccurate response of phytoplankton [*Mobley et al.*, 2015; *Penta et al.*, 2008].

To overcome the limitations associated with K_d(PAR), *Lee et al.* [2014] proposed a new radiometric term named as the usable solar radiation (USR, W m^{-2}), which is defined to represent the spectrally integrated solar irradiance

Table 1. List of Data Set, Measurements, and Number of Samples

Data Set	Measurements Used in This Study	Location	Number of Measurements (N)
South-Pacific	$-E_d(\lambda,z)$	South Pacific Gyre	36
CLT2005	$-E_d(\lambda,z)$	Chesapeake Bay	54
CLT2006	$-E_d(\lambda,z)$	Chesapeake Bay	136
CLT2007	$-E_d(\lambda,z)$	Chesapeake Bay	69
ECOMON	$-E_d(\lambda,z)$	Continental Shelf of Middle Atlantic and Gulf of Maine	25
Sortie1	$-E_d(\lambda,z)$	MOBY	30
Sortie2	$-E_d(\lambda,z)$	Scripps Pier of San Diego	17
CLV7	$-E_d(\lambda,z)$	Middle Atlantic Bight and Gulf of Maine	54

in the spectral window of 400–560 nm. Light in this window contributes the most to phytoplankton photosynthesis and can penetrate much deeper than PAR in oceanic waters, thus it is useful and important to have an accurate estimation of USR in the upper part of the global oceans.

Similarly as the description of vertical variation of PAR (equation (1)), the change of USR with depth can also be described as

$$USR(z)=USR(0^-)\cdot \exp\left[-K_d(USR)\cdot z\right] \tag{2}$$

Here $USR(0^-)$ is the subsurface downwelling usable solar radiation, while K_d(USR) is the attenuation coefficient of the downwelling USR. Based on numerical simulations by Hydrolight, *Lee et al*. [2014] found that K_d(USR) is nearly a constant vertically for almost all oceanic waters. Therefore it would be quite computationally effective for the generation of USR of the global oceans if $USR(0^-)$ and K_d(USR) are produced from satellite ocean color remote sensing. $USR(0^-)$ depends on solar elevation and atmospheric properties, which is out the scope of this study. For K_d(USR), through numerical simulations it was found that K_d(USR) of oceanic waters can be well estimated from the diffuse attenuation coefficient of downwelling irradiance at 490 nm (K_d(490), m^{-1}). But these K_d(USR) characteristics were derived purely from numerical simulations [*Lee et al*., 2014], it is important and necessary to verify these characteristics with measurements made in the real world. Here we use vertical profiles of downwelling irradiance measured in both oceanic and coastal environments to test and refine the relationships proposed in *Lee et al*. [2014]. We further produced global distribution of K_d(USR) from MODIS as examples of basin-scale satellite products.

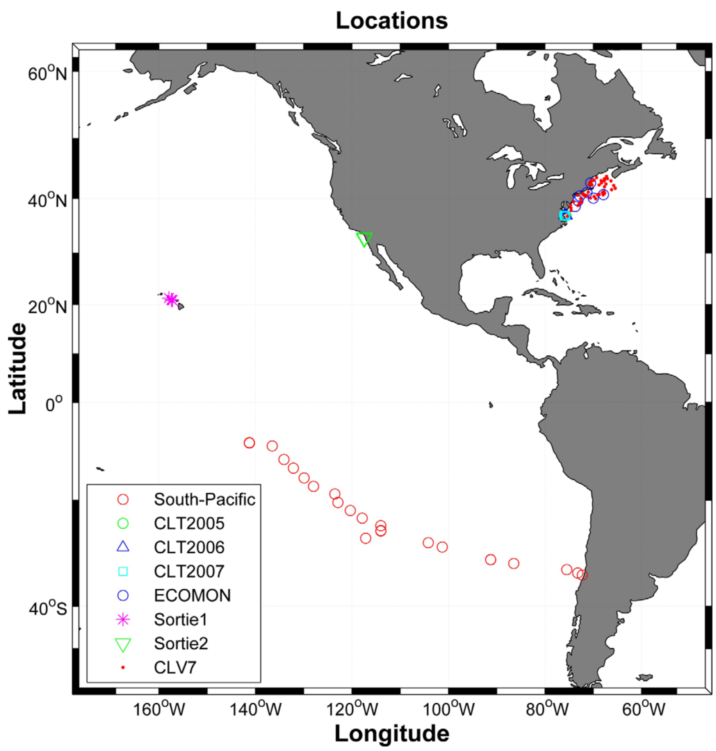

Figure 1. Locations of measurements used in this study.

2. Data and Method

2.1. Filed Measurements

The in situ data used to validate the numerical simulations consisted of eight data sets (see Table 1 and Figure 1 for summary and location, respectively) obtained from SeaBASS (http://seabass.gsfc.nasa.gov/), and all hyperspectral irradiance ($E_d(\lambda)$) measurements were obtained by Satlantic hyperspectral radiometer. Here is a brief summary of this data set.

1. The South-Pacific data set (36 $E_d(\lambda)$ profiles) collected around the South Pacific Gyre with K_d(490) in a range of ~0.017–0.14 m^{-1}. This data set represents the "clearest" natural waters on the Earth [*Claustre and Maritorena*, 2003; *Morel et al*., 2007b];

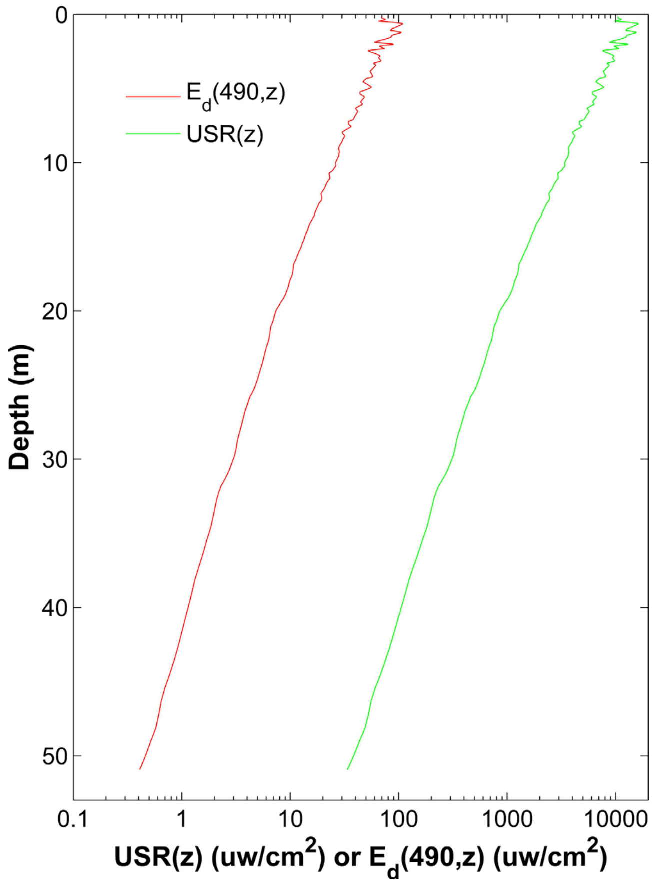

Figure 2. Example profiles of *USR* and $E_d(490)$.

2. The data set of 259 $E_d(\lambda)$ profiles obtained in the Chesapeake Bay (CLT2005, CLT2006, and CLT2007) with $K_d(490)$ varied from ~0.04 to 1.8 m^{-1};
3. The ECOMON data set of 25 $E_d(\lambda)$ profiles obtained in the continental shelf from the north of Cape Hatteras, NC to the western half of Georges Bank and a portion of the Gulf of Maine, with $K_d(490)$ in a range ~0.08–0.37 m^{-1};
4. Sortie 1 (March 2007) of 30 $E_d(\lambda)$ profiles measured at the MOBY (marine optical buoy) site with $K_d(490)$ ranging from ~0.02 to 0.31 m^{-1}; and Sortie 2 (January 2008) of 17 $E_d(\lambda)$ profiles measured at the Scripps Pier of San Diego, CA with $K_d(490)$ ranging from ~0.10 to 0.17 m^{-1}; and
5. Finally, the CLV7 data set (CLiVEC 7) of 54 $E_d(\lambda)$ profiles obtained from the cruise for the project entitled Impacts of Climate Variability on Primary Production and Carbon Distributions in the Middle Atlantic Bight and Gulf of Maine (CLiVEC), with a mean $K_d(490)$ value of ~0.15 m^{-1}.

In summary, a total of 435 downwelling $E_d(\lambda)$ (~350–700 nm, ~3 nm resolution; ~0.1 m depth resolution for most measurements) profiles were compiled from these measurements. After visually inspecting their quality, 14 measurements of $E_d(\lambda)$ profiles were removed from further analysis, because of obvious and severe random noises in the $E_d(\lambda)$ profiles that were likely due to strong wave focusing effects; therefore it leaves 421 $E_d(\lambda)$ profiles (Table 1) for this effort. Figure 2 presents an example of profiles of *USR* and $E_d(490)$ of this data set.

To evaluate how K_d(USR) changes with depth, depth-averaged K_d(USR) between 0^- and a certain depth *z*, K_d(USR, z), was computed by linear fitting the logarithm of USR(z) between 0^- and z.

$$\ln\left[USR(z)\right]=-K_d(USR,z)\cdot z+\ln\left[USR(0^-)\right] \tag{3}$$

For each station, we used a parameter, coefficient of variation (CV) of K_d(USR) (CV_{Kusr}) among the K_d(USR, z) values, to characterize the vertical variability of K_d(USR, z). CV_{Kusr} is defined as the ratio of the standard deviation to the mean value. To reduce the effect of wave focusing on the calculation of CV_{Kusr}, for each profile the first K_d(USR) was calculated from 0^- to 5% of $Z^{usr}_{1\%}$ ($Z^{usr}_{1\%}$ representing the depth where *USR*(z) is of 1% of USR(0^-)). Therefore, for each station generally more than 95% of *USR*(z) data were used to calculated K_d(USR, z) and $CV_{Kusr.}$ Additionally, averaged K_d(USR) of the upper water column is calculated by curve fitting the USR vertical profile between 0^- and $Z^{usr}_{10\%}$ with equation (3), with $Z^{usr}_{10\%}$ representing the depth where *USR*(z) is 10% of *USR*(0^-). Similarly, averaged $K_d(490)$ of the upper water column is also calculated following the same scheme.

2.2. Satellite Data

To produce sample maps of K_d(USR) of the global oceans, MODIS-Aqua monthly remote sensing reflectance (*Rrs*) with a 4 km spatial resolution was downloaded from the NASA Ocean Color website (http://

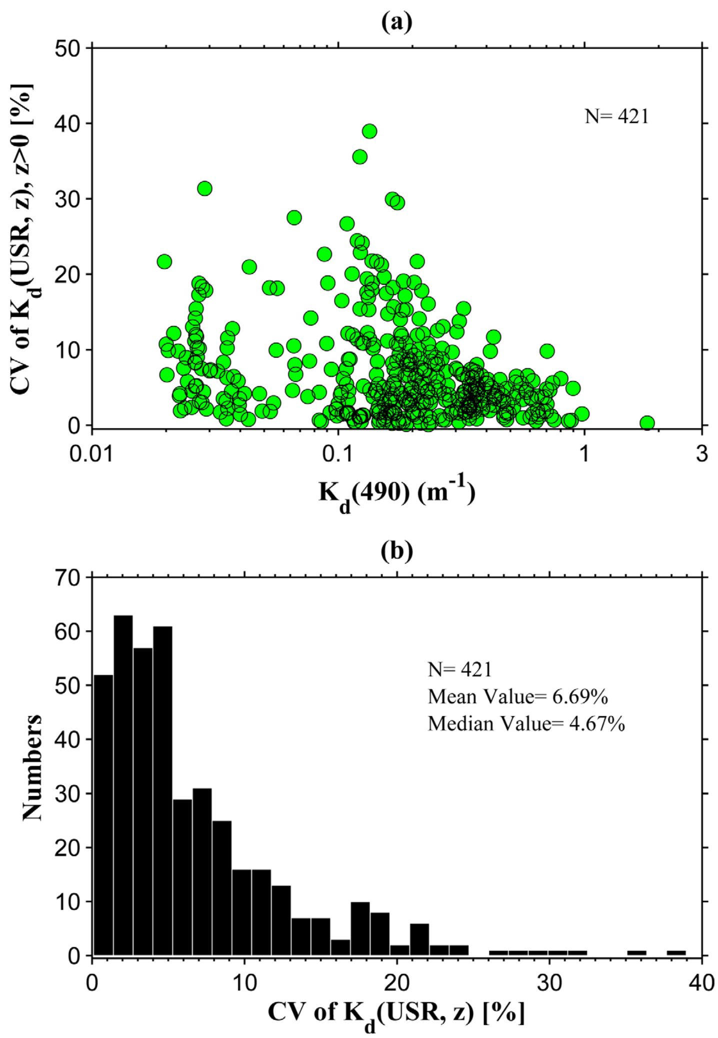

Figure 3. (a) Coefficient of variation (CV) of vertically varying attenuation coefficient (K_d(USR, z)) for all measurements; (b). Histogram of CV for all measurements.

oceancolor.gsfc.nasa.gov/). K_d(490) was estimated from the total absorption (a) and backscattering (b_b) following *Lee et al*. [2013], which were derived from *Rrs* using the quasi-analytical algorithm (QAA) [*Lee et al*., 2002]. Finally K_d(USR) was calculated from K_d(490) using the empirical model obtained in this study.

3. Results

3.1. Vertical Variability of K_d(USR)

The distribution of CV_{Kusr} from all 421 $E_d(\lambda)$ profiles is shown in Figure 3. Values of K_d(490) ranged from ~0.017 to 1.8 m^{-1} for this data set, which covers nearly the range of all natural waters. Generally, it is found that CV_{Kusr} is less than 30%, with an averaged CV_{Kusr} as 6.7%, and in particular more than 85% of the data points having CV_{Kusr} less than 12%, echoing the finding of quite uniform K_d(USR) in the upper water column [*Lee et al*., 2014]. CV_{Kusr} is found slightly larger (~8.3% on average) for K_d(490) less than 0.2 m^{-1}, probably a result of strong wave focusing effects in oceanic waters where the effect of wave focusing can reach deeper waters due to relatively low K_d(490) values. Separately, the distribution of CV of K_d(PAR) (CV_{Kpar}) from all 421 $E_d(\lambda)$ profiles is shown in Figure 4. For the same data set, the values of CV_{Kpar} generally spanned a range of ~5%–80% with an averaged CV_{Kpar} as 22.8%, and 85% of CV_{Kpar} are within ~25%. Such observations and comparisons confirm the finding in *Lee et al*. [2014] that K_d(USR, z) can be regarded as a constant vertically for oceanic waters and most turbid waters, but not K_d(PAR). Because *USR*(0^-) can be adequately generated from satellite ocean color measurements, *USR*(z) can thus be easily calculated based on equation (2) when K_d(USR) is known.

3.2. Model to Estimate K_d(USR)

A model has been developed to quickly estimate K_d(USR) with K_d(490) as the input [*Lee et al*., 2014], basically to take advantage the availability of K_d(490) as a standard product from satellite ocean color remote sensing. This empirical relationship between K_d(490) and K_d(USR) is evaluated with in situ measurements compiled in this effort. Similarly to previous studies in modeling K_d(PAR) [*Morel et al*., 2007a; *Pierson et al*., 2008; *Saulquin et al*., 2013; *Wang et al*., 2009; *Zaneveld et al*., 1993], we here used a power function to empirically describe the relationship between K_d(490) and K_d(USR) for K_d(490) >0.1 m^{-1}. On the basis of the compiled data (Table 1), it was found that K_d(USR) would be overestimated by this empirical model for K_d(490) ≤0.1 m^{-1}. The reason for such a deviation is not clear yet, although this characteristics was also found in the relationship between K_d(PAR) and K_d(490) [*Morel et al*., 2007a].

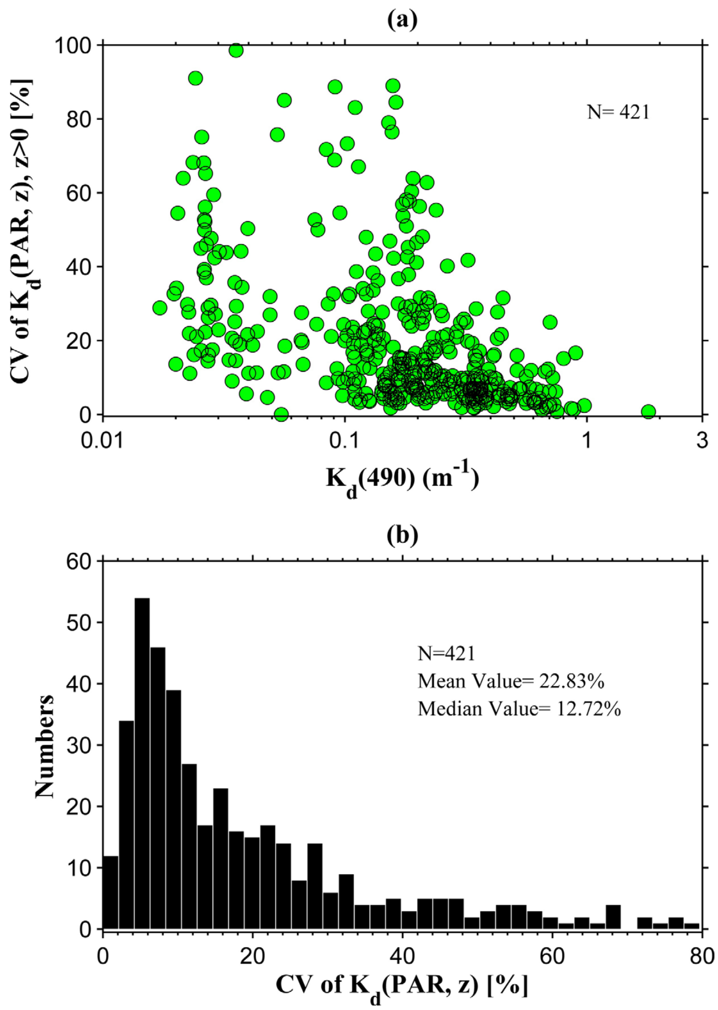

Figure 4. As Figure 3 but for K_d(PAR, z).

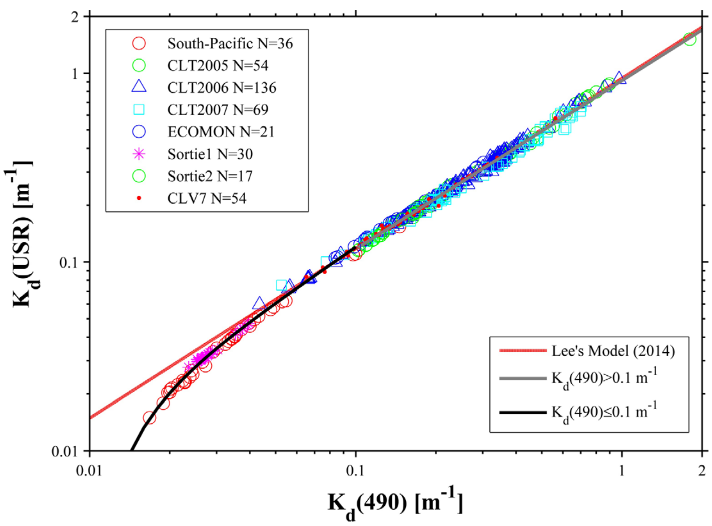

Figure 5. Models between K_d(490) and K_d(USR). The red line represents the model shown in *Lee et al.* [2014]. The gray line represents the model for $K_d(490) > 0.1$ m^{-1} and black line for $K_d(490) \leq 0.1$ m^{-1}.

Similarly to the K_d(PAR) model developed by *Morel et al.* [2007a], a two-segment model was used instead to cover waters with the lower and higher K_d(490) values (Figure 5), which is:

$$K_d(USR) = 0.91 \cdot K_d(490)^{0.89}, \quad \text{for } K_d(490) > 0.1\ m^{-1}, \quad R^2 = 0.99, MAPE = 3.2\% \tag{4a}$$

and

$$K_d(USR) = 0.0062 + 1.16 \cdot K_d(490) - 0.00018 \cdot [K_d(490)]^{-1}, \quad \text{for } K_d(490) \leq 0.1\ m^{-1}, \quad R^2 = 0.99, MAPE = 3.1\% \tag{4b}$$

where MAPE represents mean absolute percentage error ($MAPE = \frac{1}{n}\sum_{i=1}^{n}\left|\frac{x_m - x_e}{x_m}\right|$, x_m is measured value and x_e is estimated value). It was found that the model performed very well over the entire range of K_d(490) (or K_d(USR)) encountered in this study. And the model is very close to the model of *Lee et al.* [2014] for $K_d(490) > 0.1$ m^{-1}, but it differs a lot for $K_d(490) < \sim 0.04$ m^{-1} (Figure 5). This difference is likely because the synthetic data set used in *Lee et al.* [2014] has fewer data points to cover low K_d(490) values. In addition, field $E_d(\lambda)$ covered much wider range of sky conditions, but the sky radiance in the numerical simulations was set cloud free with a uniform sky, which may also affect the model parameters.

Note that both K_d(490) and K_d(USR) are apparent optical properties [*Preisendorfer*, 1976] that depend on the angular distribution of the light field [*Kirk*, 1991; *Smith et al.*, 1989]. However, the interrelationship

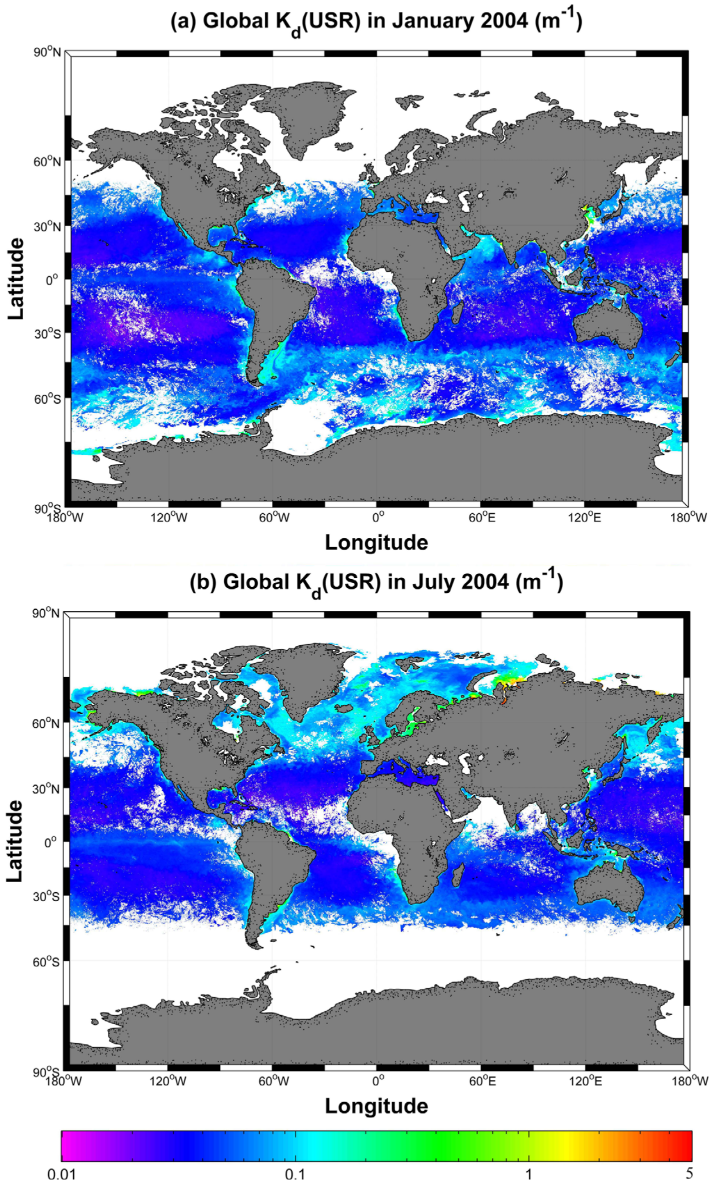

Figure 6. Distribution of K_d(USR) of the global oceans for the months of January and July 2004, respectively.

between K_d(USR) and K_d(490), as indicated in *Lee et al.* [2014], is rather insensitive to the sun zenith angle. Such a result provides a confidence in applying the model of equation (4a) to various light conditions.

4. Distribution of K_d(USR) of Global Oceans and Its Implications

As examples, global distributions of K_d(USR) for January and July 2004 (see Figure 6) were produced by equation (4), respectively, from MODIS monthly composites of *Rrs*, with K_d(490) derived from *a* and b_b using the K_d model developed by *Lee et al.* [2013], and *a* and b_b calculated from *Rrs* using QAA [*Lee et al.*, 2002]. As expected, K_d(USR) of the global oceans has minimum values ($\sim$0.02 m^{-1}) in the ocean gyres, while much higher values (as high as $\sim$5.2 m^{-1}) for coastal turbid waters. There are also clear seasonal variations in K_d(USR) for both oceanic and coastal regions.

Historically, the euphotic zone depth (Z_{eu}) is used to represent the layer of water where net photosynthesis is positive. The practical definition of Z_{eu} is the depth where 1% of the surface PAR remains [*Kirk*, 1994; *Siegel et al.*, 2001]. Z_{eu} is not only a quality index of water clarity [*Shang et al.*, 2011], used in some production models [*Arrigo et al.*, 1998; *Behrenfeld and Falkowski*, 1997], also an important parameter to get the integrated primary production of the water column. By definition, PAR is the spectrally integrated radiation in the 400–700 nm range, but the photons in the 600–700 nm range quickly disappear in the upper few meters, thus only a portion of the surface PAR actually reaches deeper depths. USR, on the other hand, represents photons in the blue-green domain that are most important for phytoplankton photosynthesis and photooxidation of color dissolved organic matter (CDOM) [*Osburn and Morris*, 2003]. It is thus interesting to know the difference between the penetration depth of *USR* (Z_{eu}^{usr}) and the penetration depth of *PAR* (Z_{eu}^{par}).

Similarly as the definition of the euphotic zone depth of PAR, we here define Z_{eu}^{usr} as the depth where 1% of surface USR remains. With known K_d(USR), $Z_{eu}^{usr} = 4.6/K_d$(USR) (the value 4.6 comes from $-\ln(0.01)$), and the global distributions of Z_{eu}^{usr} of January and July of 2004, respectively, are presented in Figure 7. It is found that large portions of the oceans having Z_{eu}^{usr} in a range of 100–250 m. For comparison Z_{eu}^{par} is

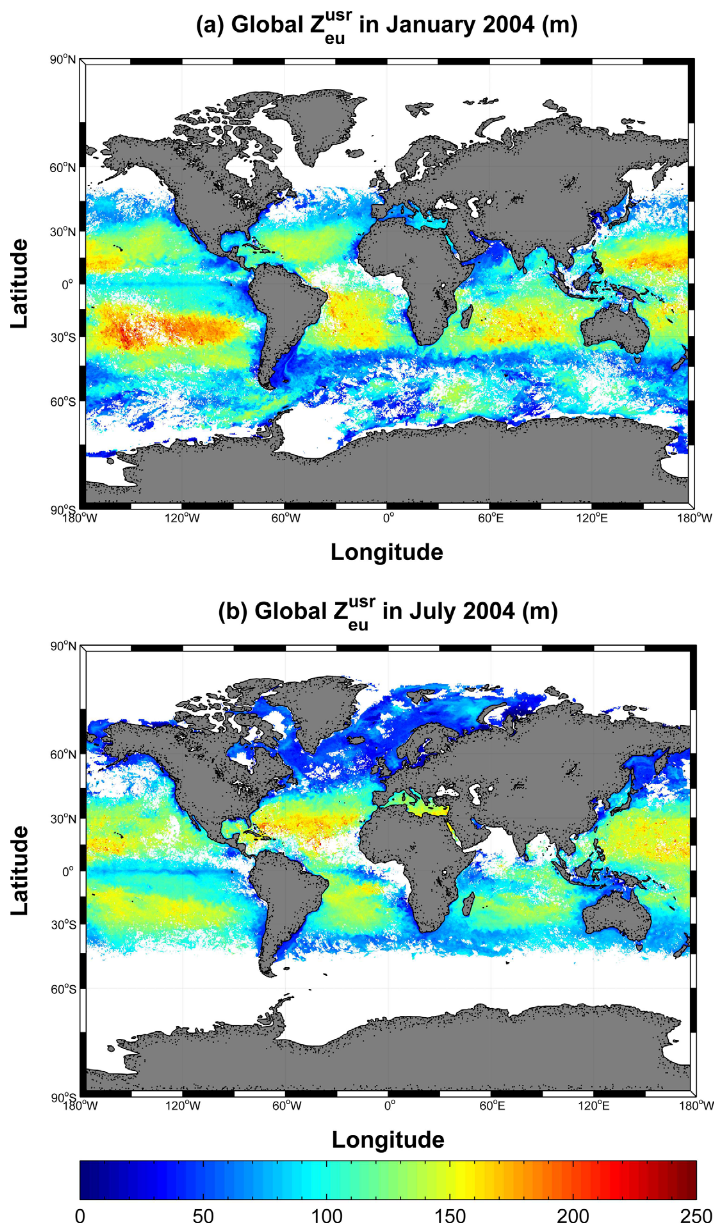

Figure 7. Distribution of Z_{eu}^{usr} of the global oceans for months of January and July 2004, respectively.

estimated from $Z_{eu}^{par} = 4.6/K_d(\text{PAR})$, with K_d(PAR) calculated from K_d(490) following the K_d(490)-K_d(PAR) relationship of *Morel et al*. [2007a]. Figure 8 shows the global distribution of the depth difference between Z_{eu}^{usr} and Z_{eu}^{par} ($Z_{eu}^{usr}-Z_{eu}^{par}$). It is found that the largest difference (~100 m) between Z_{eu}^{usr} and Z_{eu}^{par} occurs in ocean gyres (Figure 8). For some turbid inland and estuarine waters, since it is the shorter wavelengths contribute most to both K_d(PAR) and K_d(USR), the difference between Z_{eu}^{usr} and Z_{eu}^{par} tends to be small.

Normally surface USR is about 0.65 of surface PAR. If *PAR*(0) is 1 Einst/m^2/d, the above results indicate that for a water body with Z_{eu}^{usr} as 250 m there are still 1% USR at 250 m, but it is ~0.08% of surface PAR at this depth if it is estimated based on the model of a vertically constant K_d(PAR) (equation (1)). This is an increase of about seven folds of photons at such a depth, and these "new found light" may help to explain the deep chlorophyll max (e.g., at ~195 m) [*Morel et al*., 2007b] found in the oceanic waters. These results suggest that the redefined depth Z_{eu}^{usr} likely better represents the term "euphotic zone depth" of photosynthesis than Z_{eu}^{par} [*Marra et al*., 2014]. Note that the underestimation of solar radiation at depths by the traditional K_d(PAR) approach is mainly due to the incorrect assumption of a vertically constant K_d(PAR) [*Lee*, 2009; *Morel*, 1988]. In addition to the use of K_d(USR), an accurate estimation of solar radiation at depths could also be achieved following a more complex approach of *Lee et al*. [2005], where the attenuation coefficient of visible solar radiation is modeled as a function of depth.

Further, the primary production of phytoplankton can be estimated from photosynthetic utilizable radiation (PUR) [*Morel*, 1978], and an empirical relationship between *PUR*(z) and *USR*(z) has been developed [*Lee et al*., 2014]. Since *USR*(z) can be easily estimated from *USR*(0^-) and K_d(USR) (equation (2)) and *USR*(0^-) is estimated based on sun angle and atmosphere properties, the production and availability of K_d(USR) provides a simple, and reasonably accurate, approach to reduce the complexity in calculating absorbed energy in the upper water column for photosynthesis of the global oceans [*Cullen et al*., 2012].

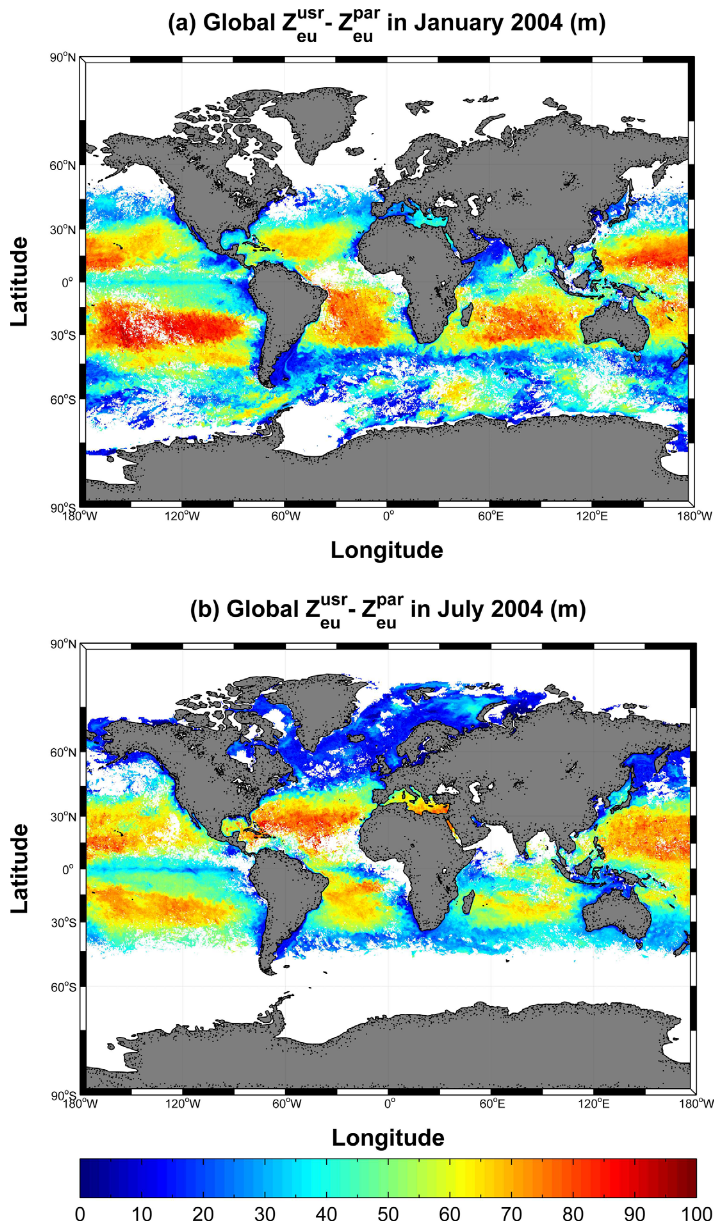

Figure 8. Distribution of the difference between Z_{eu}^{usr} and Z_{eu}^{par} ($Z_{eu}^{usr} - Z_{eu}^{par}$, $Z_{eu}^{par} = 4.6/K_d(\mathrm{PAR})$) of the global oceans for months of January and July 2004, respectively.

5. Summary

Using filed measurements covering a wide range of water properties, it is found that K_d(USR) can be regarded as a constant vertically in the upper water column for both clear and many "turbid" waters. This is consistent with the results shown in *Lee et al*. [2014] for clear waters ($K_d(490) <$ 0.2 m^{-1}) developed purely from numerical simulations. Further, we refined the relationship between K_d(USR) and K_d(490) proposed in *Lee et al*. [2014] based on the field measurements that include data of the "clearest" natural waters. This new relationship can then be applied to waters from very clear ocean gyres to turbid coastal regions, and as examples global distributions of K_d(USR) were produced from MODIS-Aqua measurements. It is found that the minimum K_d(USR) is ~0.02 m^{-1} in ocean gyres, while the maximum K_d(USR) is ~5.2 m^{-1} for turbid coastal waters, along with clear seasonal variations. These K_d(USR) distributions indicate that there are still many photons even at ~250 m for oceanic gyres, which is significantly deeper than the conventionally perceived euphotic zone depth of such waters (~180 m). This characteristic may help to explain the reported deep chlorophyll maximum at such depths in the ocean gyres.

Acknowledgments
This study was supported by NASA (grant NNX14AM15G). We thank SeaBASS and all the contributors of field measured data (http://seabass.gsfc.nasa.gov/). Comments and suggestions from two anonymous reviewers are greatly appreciated.

References

Arrigo, K. R., D. Worthen, A. Schnell, and M. P. Lizotte (1998), Primary production in Southern Ocean waters, *J. Geophys. Res.*, *103*(C8), 15,587–15,600.

Behrenfeld, M. J., and P. G. Falkowski (1997), A consumer's guide to phytoplankton primary productivity models, *Limnol. Oceanogr.*, *42*(7), 1479–1491.

Buiteveld, H. (1995), A model for calculation of diffuse light attenuation (PAR) and Secchi depth, *Neth. J. Aquat. Ecol.*, *29*(1), 55–65.

Claustre, H., and S. Maritorena (2003), The many shades of ocean blue, *Science*, *302*(5650), 1514–1515.

Cullen, J. J., R. F. Davis, and Y. Huot (2012), Spectral model of depth-integrated water column photosynthesis and its inhibition by ultraviolet radiation, *Global Biogeochem. Cycles*, *26*, GB1011, doi:10.1029/2010GB003914.

Frouin, R., and R. T. Pinker (1995), Estimating photosynthetically active radiation (PAR) at the earth's surface from satellite observations, *Remote Sens. Environ.*, *51*(1), 98–107.

Frouin, R., J. McPherson, K. Ueyoshi, and B. A. Franz (2012), A time series of photosynthetically available radiation at the ocean surface from SeaWiFS and MODIS data, Proc. SPIE 8525, Remote sensing of the Marine Environment II.

Kara, A. B., A. J. Wallcraft, and H. E. Hurlburt (2005), Sea surface temperature sensitivity to water turbidity from simulations of the Turbid Black Sea using HYCOM, *J. Phys. Oceanogr.*, *35*(1), 33–54.

Kirk, J. T. (1991), Volume scattering function, average cosines, and the underwater light field, *Limnol. Oceanogr.*, *36*(3), 455–467.
Kirk, J. T. (1994), *Light and Photosynthesis in Aquatic Ecosystems*, Cambridge Univ. Press.
Lee, Z. (2009), K_{PAR}: An optical property associated with ambiguous values, *J. Lake Sci.*, *21*(2), 159–164.
Lee, Z., K. L. Carder, and R. A. Arnone (2002), Deriving inherent optical properties from water color: A multiband quasi-analytical algorithm for optically deep waters, *Appl. Opt.*, *41*(27), 5755–5772.
Lee, Z., K. Du, R. Arnone, S. Liew, and B. Penta (2005), Penetration of solar radiation in the upper ocean: A numerical model for oceanic and coastal waters, *J. Geophys. Res.*, *110*, C09019, doi:10.1029/2004JC002780.
Lee, Z., C. Hu, S. Shang, K. Du, M. Lewis, R. Arnone, and R. Brewin (2013), Penetration of UV-visible solar radiation in the global oceans: Insights from ocean color remote sensing, *J. Geophys. Res. Oceans*, *118*, 4241–4255, *doi*:10.1002/jgrc.20308.
Lee, Z., S. Shang, K. Du, J. Wei, and R. Arnone (2014), Usable solar radiation and its attenuation in the upper water column, *J. Geophys. Res. Oceans*, *119*, 1488–1497, doi:10.1002/2013JC009507.
Marra, J. F., V. P. Lance, R. D. Vaillancourt, and B. R. Hargreaves (2014), Resolving the ocean's euphotic zone, *Deep Sea Res. Part I*, *83*, 45–50.
McCree, K. J. (1981), Photosynthetically active radiation, in *Physiological Plant Ecology I*, edited by O. L. Lange et al., pp. 41–55, Springer, Berlin.
Mobley, C. D., F. Chai, P. Xiu, and L. K. Sundman (2015), Impact of improved light calculations on predicted phytoplankton growth and heating in an idealized upwelling-downwelling channel geometry, *J. Geophys. Res. Oceans*, *120*, 875–892, doi:10.1002/2014JC010588.
Morel, A. (1978), Available, usable, and stored radiant energy in relation to marine photosynthesis, *Deep Sea Res.*, *25*(8), 673–688.
Morel, A. (1988), Optical modeling of the upper ocean in relation to its biogenous matter content (case I waters), *J. Geophys. Res.*, *93*(C9), 10,749–10,768.
Morel, A., Y. Huot, B. Gentili, P. J. Werdell, S. B. Hooker, and B. A. Franz (2007a), Examining the consistency of products derived from various ocean color sensors in open ocean (Case 1) waters in the perspective of a multi-sensor approach, *Remote Sens. Environ.*, *111*(1), 69–88.
Morel, A., B. Gentili, H. Claustre, M. Babin, A. Bricaud, J. Ras, and F. Tieche (2007b), Optical properties of the "clearest" natural waters, *Limnol. Oceanogr.*, *52*(1), 217–229.
Murtugudde, R., J. Beauchamp, C. R. McClain, M. Lewis, and A. J. Busalacchi (2002), Effects of penetrative radiation on the upper tropical ocean circulation, *J. Clim.*, *15*(5), 470–486.
Osburn, C. L., and D. P. Morris (2003), Photochemistry of chromophoric dissolved organic matter in natural waters, in *UV Effects in Aquatic Organisms and Ecosystems*, vol. 1, edited by E. W. Helbling and H. Zagarese, pp. 185–217, Royal Society of Chemistry, Cambridge.
Paulson, C. A., and J. J. Simpson (1977), Irradiance measurements in the upper ocean, *J. Phys. Oceanogr.*, *7*(6), 952–956.
Penta, B., Z. Lee, R. M. Kudela, S. L. Palacios, D. J. Gray, J. K. Jolliff, and I. G. Shulman (2008), An underwater light attenuation scheme for marine ecosystem models, *Opt. Express*, *16*(21), 16,581–16,591.
Pierson, D. C., S. Kratzer, N. Strömbeck, and B. Håkansson (2008), Relationship between the attenuation of downwelling irradiance at 490 nm with the attenuation of PAR (400 nm–700 nm) in the Baltic Sea, *Remote Sens. Environ.*, *112*(3), 668–680.
Preisendorfer, R. (1976), *Hydrologic optics. Vol. I. Introduction*, U.S. Dep. of Commer., Natl. Oceanic and Atmos. Admin., Environ. Res. Lab., Honolulu, Hawaii.
Saulquin, B., A. Hamdi, F. Gohin, J. Populus, A. Mangin, and O. F. d'Andon (2013), Estimation of the diffuse attenuation coefficient K dPAR using MERIS and application to seabed habitat mapping, *Remote Sens. Environ.*, *128*, 224–233.
Shang, S., Z. Lee, and G. Wei (2011), Characterization of MODIS-derived euphotic zone depth: Results for the China Sea, *Remote Sens. Environ.*, *115*(1), 180–186.
Siegel, D., T. Westberry, M. O'brien, N. Nelson, A. Michaels, J. Morrison, A. Scott, E. Caporelli, J. Sorensen, and S. Maritorena (2001), Bio-optical modeling of primary production on regional scales: The Bermuda BioOptics project, *Deep Sea Res. Part II*, *48*(8), 1865–1896.
Smith, R., J. Marra, M. Perry, K. Baker, E. Swift, E. Buskey, and D. Kiefer (1989), Estimation of a photon budget for the upper ocean in the Sargasso Sea, *Limnol. Oceanogr.*, *34*(8), 1673–1693.
Wang, M., S. Son, and L. W. Harding (2009), Retrieval of diffuse attenuation coefficient in the Chesapeake Bay and turbid ocean regions for satellite ocean color applications, *J. Geophys. Res.*, *114*, C10011, doi:10.1029/2009JC005286.
Zaneveld, J. R. V., J. C. Kitchen, and J. L. Mueller (1993), Vertical structure of productivity and its vertical integration as derived from remotely sensed observations, *Limnol. Oceanogr.*, *38*(7), 1384–1393.